

Performance of solar PV-fuel cell (FC) hybrid system for stand-alone applications

T. Ramesh^{1*}, L. Dharunprasath², S. Kaliappan³, G. Emayavaramban⁴

¹Department of EEE, Karpagam Academy of Higher Education, Coimbatore.

²Department of EEE, Karpagam Academy of Higher Education, Coimbatore.

³Department of EEE, Kumaraguru College of Technology, Coimbatore.

⁴Assistant Professor, Department of EEE, Karpagam Academy of Higher Education, Coimbatore.

*Corresponding author E-mail: your.ramesh83@gmail.com

Abstract

This paper presents the performance of a hybrid solar PV/ Fuel Cell/ FC system with a PMDC motor load. The hybrid system supplies power to the DC motor during day and night. In order to obtain continuous supply to the load, a control strategy is implemented in the system. By using this control strategy, the solar PV and the fuel cell supply the voltage to the load by getting constant supply from the DC link during day and night. The DC-DC interleaved soft switching boost converter (ISSBC) with Incremental conductance maximum power point tracking technique (INC MPPT) is used to maintain constant DC link voltage. When the power deficit happens in the solar PV, the hydrogen stored in the tank is used by the fuel cell stack and supplies power to the load. The entire system is modeled and the performance of the hybrid system is analyzed in MATLAB/Simulink environment.

Keywords: Solar PV, PEM fuel cell, DC-DC interleaved soft switching boost converter (ISSBC), PMDC motor, matlab/simulink, embedded matlab.

1. Introduction

From the last decades, increasing amount of industrial growth, hasty reduction of fossil fuel resources, their unstable prices, rapid rise of energy demand due to increasing population, CO₂ emission and environment pollution due to fossil fuel turns the interest into developing renewable energy sources such as solar PV, wind, bio gas, and fuel cell which lead clean energy to implement from small scale applications to grid parity applications. The total use of renewable energy sources in the worldwide is 6.4% as on 2011 [1] Recently, hybrid system using renewable energy sources is used to fulfill the vast energy demand in rural and remote areas such as radio telecommunications and satellite earth stations. Hybrid energy systems are more attractive and chosen as alternative energy sources where the power supply needed area is far away from the non renewable energy sources [2- 4]. Among them, some of the resources are highly stochastic and site-specific [5]. For example, wind is a site-specific energy source and also the wind velocity and speed could not be predicted because, which is always changing [6]. The problem associated with PV generation system is that the conversion efficiency is low due to low irradiations. The conversion from sunlight into electricity also varies because it entirely depends on climatic conditions such as solar irradiation and cell temperature [7]. In this work, a hybrid system using solar PV and Proton Exchange Membrane fuel cell (PEM) is used to obtain higher efficiency and that could be obtained from the single source. Solar PV system combined with fuel cell presents flexible system, less maintenance, easily adopts in any location, particularly pollution free [8]. This rest of the paper is organized into following sections as follows. The section 2 describes the proposed system if this work. Section 3 explains hybrid system configuration. Section 4 illustrates result and

discussion of the proposed work using MATLAB/Simulink. In section 5 conclusion of the work is presented.

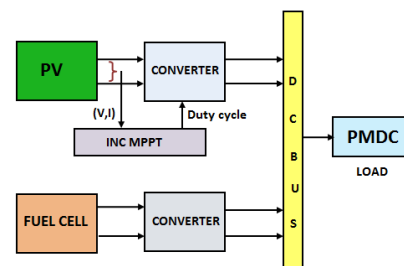


Figure 1: System block diagram

2. The proposed system

Overall system description

Hybrid PV and fuel cell with Permanent Magnet Direct Current (PMDC) motor load as show Figure 1. Grid connected system need not store power. i.e., backup system is not necessary. Standalone system needs a backup system to fulfill the demand during night as well when the PV source could not generate power. For that reason, fuel cells are used as backup system, when there is no solar irradiation or low solar irradiation.

3. Hybrid system configuration

Solar PV module

BP SX 150S PV module is selected for MATLAB simulation using Embedded MATLAB. The PV cell is made up of multi-

crystalline silicon which has 72 cells connected in series and delivers 150 W nominal maximum power at standard test conditions 1 suns where 1 suns=1000 W/ m².

Solar PV cell model

In this work, the single diode model with R_s is used to study the characteristics of solar PV module [9, 10]. The equivalent circuit diagram is shown in Figure 2. From the theory of semiconductor devices, the following equation mathematically describes the I-V characteristics of the PV cell:

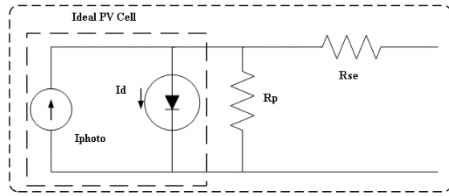


Figure 2: Equivalent model of the PV panel

The series resistance R_{se} and parallel resistances R_p represents the non-idealities. The basic current equation is given in Equation (1).

$$I = I_{pv} - I_0 \left[\exp \frac{qV}{AkT} - 1 \right] \tag{1}$$

where,

- I_{PV} - current generated by the incident light
- T - Temperature of the PN junction
- A - Diode ideality constant
- I₀ - leakage current of the diode
- q - electron charge 1.6021×10⁻¹⁹ C
- k - Boltzmann constant (1.38×10⁻²³ J/K)

Table 1: BP SX 150S PV Module Electrical Characteristics

Parameters	Value
Maximum Power (P _{max})	150W
Voltage at Pmax (V _{mp})	34.5V
Current at Pmax (I _{mp})	4.35A
Open-circuit voltage (V _{oc})	43.5V
Short-circuit current (I _{sc})	4.75A

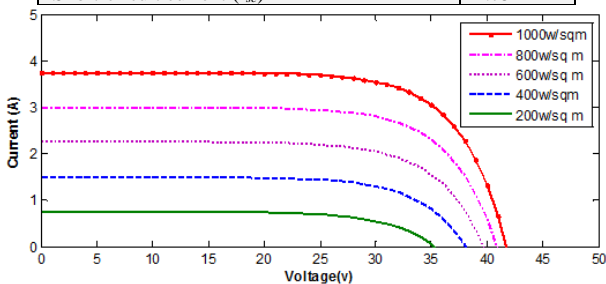


Figure 3: V-I curves of BPSX 150s PV module at various irradiances

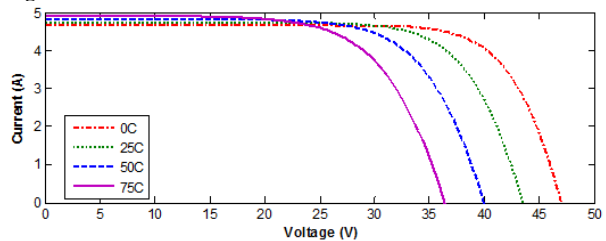


Figure 4: I-V curves of BPSX 150s PV module at various temperatures
The Equation (1) represents the basic equation of ideal photovoltaic cell. A single PV cell produces an output voltage of less than 1 volt, hence practically more number of PV cell are connected in series to achieve a desired output voltage. PV panel I-V characteristic AT various insulation and temperature shown in figure 3 and figure 4 respectively.

4. Classification of MPPT algorithms

The objective of MPPT algorithm is to draw maximum power from PV modules for changing solar irradiance and temperature circumstances or when the solar panel is partially shaded. With that aim, PV modules impedance (source) is matched to the load impedance and maximum power generation is ensured. For a fixed load, the equivalent impedance seen by the panel can be adjusted by changing the power converter duty cycle discussed; Figure 5 illustrates the PV system equivalent circuit and the input impedance concept.

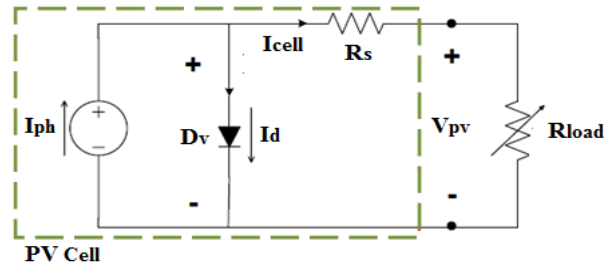


Figure 5: Equivalent circuit of PV cell

By definition Zhou et al (2010) a maximum power point tracking (MPPT) control mutual to a ISSBC converter allows a photovoltaic initiator to produce the maximum constant power, whatsoever the metrological conditions (irradiance, temperature). Energy conversion efficiency of MPPT algorithm is calculated by the Equation (2).

$$\eta_{MPPT} = \frac{\int_0^t P_{pv-max}(t) dt}{\int_0^t P_{pv-mppt}(t) dt} \tag{2}$$

where P_{pv-mppt} represents the output power of PV with MPPT, P_{pv-max} is the actual output power at maximum power point.

In MPPT controller, duty cycle is the control parameter. The MPPT controller tune the duty cycle (α) to its optimal value under variations in solar irradiance and temperature. The MPPT circuit consists of power circuit and the regulator. The two configurations of MPPT method are the input voltage V_{pv} and current I_{pv} are used for MPP tracking. In this container, the duty cycle (α) is endlessly tuned until the MPP is reached.

Incremental conductance

This method focuses directly on power variations. This method tracks the maximum power point by comparing the solar array incremental conductance (ΔG=dI_{pv}/dV_{pv}) and direct conductance (G=I_{pv}/V_{pv}), the purpose of this procedure is explained in the flowchart in Figure 6. The PV panel voltage and current are deliberate at unchanging sampling intervals and fed to the controller to compute the PV panel power. The PV panel incremental conductance is conventional by measuring diminutive changes in array voltage and current. The PV panel instant conductance is calculated by dividing the array current by the voltage. The aim of this algorithm is to track the voltage operating point at which conductance is equal to incremental conductance. Hence,

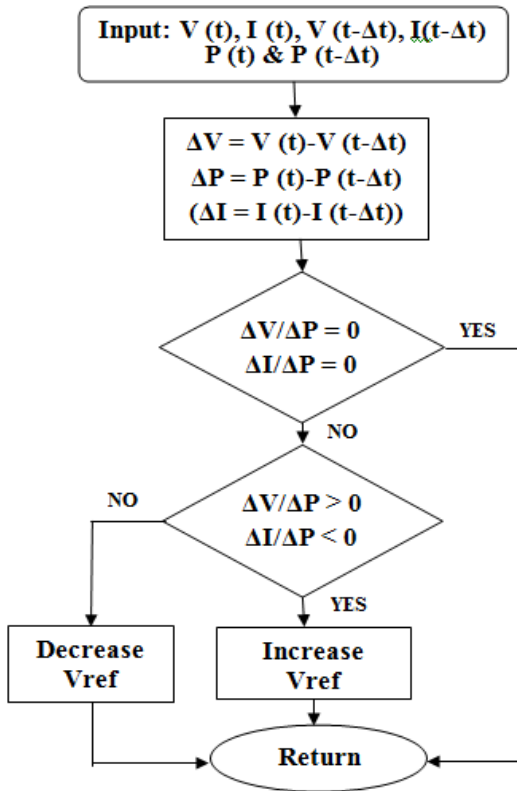


Figure 6: Incremental conductance algorithms

$$\left. \begin{aligned} \frac{dP_{pv}}{dV_{pv}} = 0 & \quad \frac{I_m}{V_m} = -\frac{\Delta I_{pv}}{\Delta V_{pv}} & G = \Delta G \\ \frac{dP_{pv}}{dV_{pv}} > 0 & \quad \frac{I_m}{V_m} > -\frac{\Delta I_{pv}}{\Delta V_{pv}} & G > \Delta G \\ \frac{dP_{pv}}{dV_{pv}} < 0 & \quad \frac{I_m}{V_m} < -\frac{\Delta I_{pv}}{\Delta V_{pv}} & G < \Delta G \end{aligned} \right\} \quad (3)$$

It works under varying solar irradiance and temperature. INC method requires more calculations than P&O method convergence is slow. The INC method used to have complex analog implementation but it is easier nowadays with micro controllers [13]. However, the INC method requires more calculations than P&O method and thus slows down the sampling speed [6], [12], [14]. Finally, the null value of the slope of the PV array power versus voltage curve seldom occurs [6]

DC-DC interleaved boost soft switching Converter

Basic operation ISSBC

Figure 7 shows the circuit diagram of ISSBC, it consists of two single-phase boost inverters that are related in parallel and inverters in service 180 degree out of phase with 30 kHz switching incidence. Interleaved converter mode 60 kHz result is achieved by phase changing of the two 30 kHz switching signals [20]. Because the inductor ripples currents are absent of phase, they call off each other and the input-ripple current diminish to 12% of that of a conventional boost converter, because the input current is the amount of each current of inductor L1 and L2. The best input-inductor-ripple-current crossing out occurs at 50% duty cycle shown in Figure 8. Therefore, the interleaved converter have the wider nonstop current mode, the condensed input current ripple and output voltage ripple, and lower switching losses, therefore the output voltage of the solar cell can be boosted with high effectiveness.

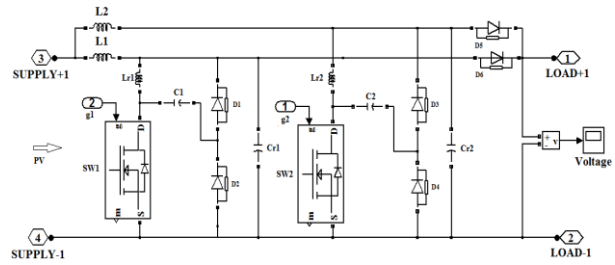


Figure 7: Circuit diagram of ISSBC

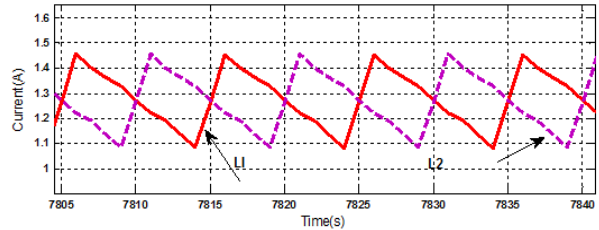


Figure 8: ISSBC Main inductor L1 and L2 current simulated waveform

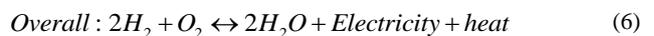
It serves as a suitable interface for PV cells to convert low voltage high current input into a high voltage low current output. The advantages of interleaved boost converter compared to the classical boost converter are low input current ripple, high efficiency, and faster transient response, reduced electromagnetic emission and improved reliability, therefore the output voltage of the solar cell can be boosted with high efficiency

Fuel cell

In order to meet the power needs, the fuel cells play a promising role to fulfill the energy demand. Fuel cell is a device where hydrogen reacts with oxygen to produce water and heat and the electron at the anode flows through the external circuit to produce electric current through electrochemical process. Due to poor pollutant emissions, particularly green house gases / NOx, SOx, and CO2, fuel cells are more attractive energy source which can be integrated with other non renewable energy sources. Among the various fuel cell types listed in [13], the PEM fuel cells are most commonly used in automotive applications because it can be operates at very low temperature as below 100°C, the PEM fuel cell have smaller in volume a bed weight due to high power density which will lead less maintenance [13].

Basic operation of PEM fuel cell

PEM fuel cell is a nonlinear, several-input and -output, powerfully coupled, and large delay dynamic system [14]. The PEM fuel cell mostly uses fuel as hydrogen and oxidant as oxygen. The oxidant may be air. These gases should be wet to prevent dehydration. A single fuel cell will produce 0.6 V. All fuel cells connected together to produce required electrical power and voltage. This PEM cell is mainly suitable for highly distributed applications. The basic operation of the PEM fuel cell is as follow:



MATLAB/Simulink environment is used to model the fuel cell. This model is embedded in to Sim power system of MATLAB. From Figure 6, the output voltage of the single fuel cell can be distinct by the following appearance:

$$V_{PEMFC} = E_{Nernst} - V_{act} - V_{ohmic} - V_{con} \quad (7)$$

Where, E_{Nernst} is the thermodynamic potential of the cell and it represents its reversible voltage V_{act} is the voltage drop associated with the activation of anode and cathode V_{ohmic} is the voltage drop ensuing from the resistance of the conduction of proton during the solid membranes and the electrons throughout its path V_{con} is the voltage drop linked with the decrease in the absorption of reactants gases or mass transportation of reactants.

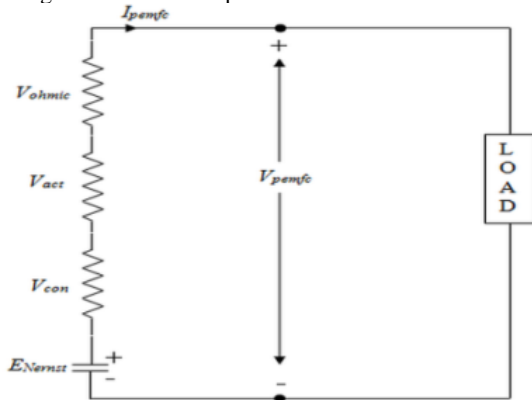


Figure 9: Electrical equivalent circuit of PEM fuel cell

Electrolyzer Model

For commercial electrolyzer, the empirical model in Eq. (8) is used at known operating temperature for simulation in [15].

$$V = n_c V_{rev} + a \left(\frac{I}{A} \right) + b \log \left[c \left(\frac{I}{A} \right) + 1 \right] \quad (8)$$

Where V is the cell operating Voltage/V. V_{rev} is reversible cell voltage/V, a is the ohmic resistance of electrolyte/ Im^2 and b & c are the coefficients of overvoltage on electrodes, A area of electrode/ m^2 , I is the current through the cell/A and n_c is the number of cells in stack. Coefficients a, b, c are the functions of temperature. In order to find the above coefficients curve fitting method by using Matlab is used from the experimental data from [16]. The obtained values are substituted in Eq. (7) exhibit the cell operating voltage is as follows: The Eq. (6) is used as electrolyzer model for simulation in this work.

Permanent magnet dc motor

An ideal DC motor equivalent circuit model is shown in Figure 10

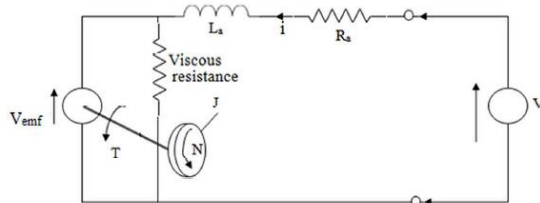


Figure 10: PMDC motor equivalent circuit

$$V = R_a + L_a \frac{di}{dt} + V_{emf} \quad (9)$$

The motor output voltage is calculated using Kirchoff's voltage law as Where; R_a , L_a and V_{emf} are armature resistance, inductance and back emf, respectively.

Results and discussion

Table 1 list out the electrical specification of 150 Watts solar PV panel provided by the manufacturer. The modeling of PV cell is simulated using Embedded Matlab function and is shown in Figure 11. In order to study the characteristics of solar PV panel, embedded MATLAB function is used in the simulation as shown

in Figure 11. The panel is simulated for analyzing P-V and I-V characteristics at standard test conditions and the MPP (Maximum Power Point) occurs at 150 W. Here the voltage is 35 V and current is 4.8 A as given in Figure 12. Using the Eq. (9), the modeling of fuel cell is performed using MATLAB/Simulink.

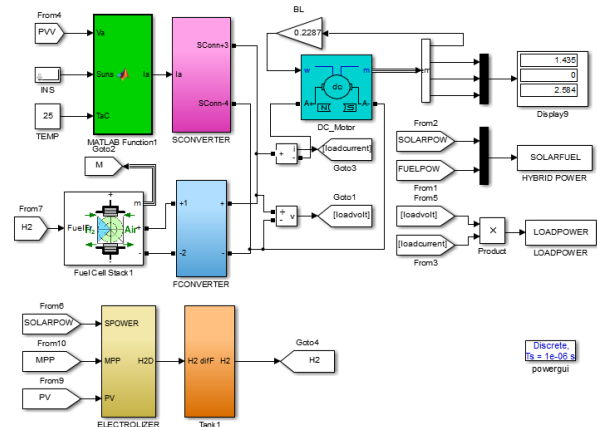


Figure 11: MATLAB/simulink diagram of the Solar PV/Fuel Cell with PMDC motor

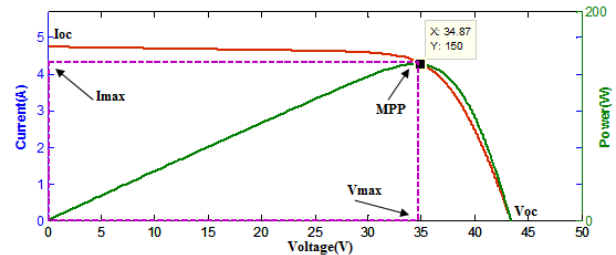
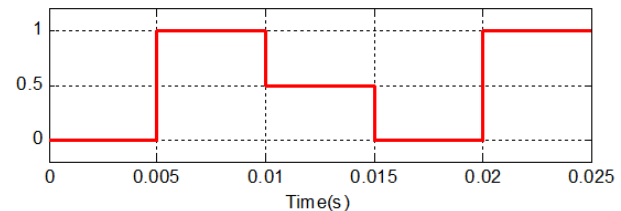


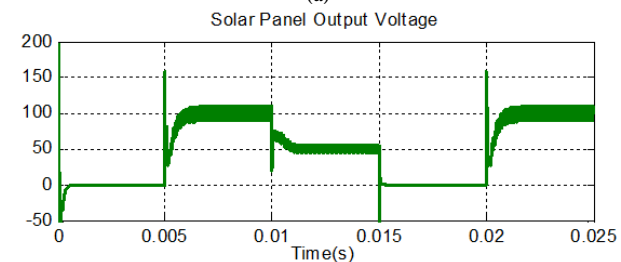
Figure 12

Case 1

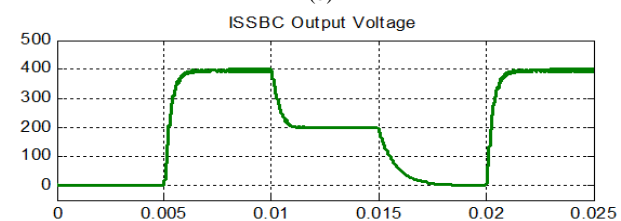
First the hybrid system performance analysis different insulation condition of the PV panel found the panel output and ISSBC output voltage. The insulation '0' is considered night, '1' is considered as day and '0.5' is considered as partial shaded condition. The simulated response of PV, ISSBC, fuel cell and hybrid voltage shown in figure 13 (a-e). Insolation (W/msq)



(a)



(b)



(c)

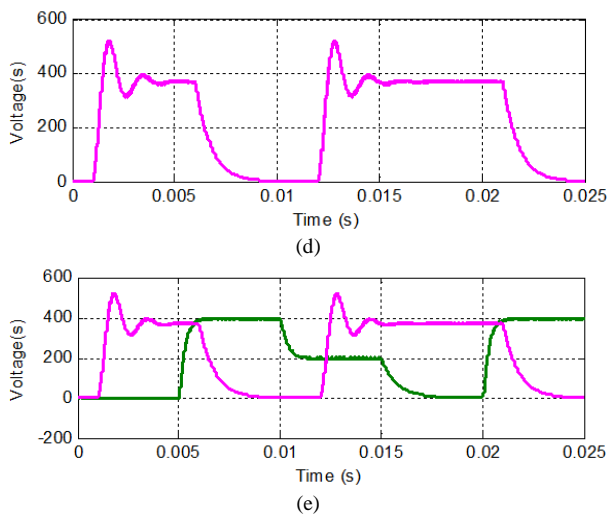


Figure 13: Performance of solar PV and fuel cell at 25° C (a) insolation,(b) PV voltage (c) ISSBC voltage,(D) Fuel cell voltage,(e) Hybrid of solar and fuel cell

Case 2

Figure 14 (a-e) shows MATLAB/Simulink circuit for the hybrid system used in this work for performance analysis. The proposed solar hybrid system is simulated for two irradiation values i.e., 0 and 1 suns. The 0 is considered as night and 1 as day. At night, the supply to the motor is fed through fuel cell stack. The insolation changes from 0 to 1 suns, and the power is increased in the solar PV. When the solar power is greater than 50W, the fuel cell shuts down, and supply to the load is fed by solar PV. The Figure 14 shows the irradiation set as 0 suns that is no irradiation up to 0.01 seconds. After 0.01 seconds, the irradiation is set as 1 suns. There is no irradiation i.e., 0 suns, from 0 to 0.01 sec, and also, the fuel cell supplies power to the load. After 0.01 seconds, the insolation is 1 suns, the solar PV supplies power to the load. When the solar PV power reaches above the load demand, the remaining power is supplied to the electrolyser which produces fuel. For both the cases, the solar cell temperature is maintained as 25°C. The power supplied to the load by both fuel cell and solar PV. The PMDC motor gets continuous supply from fuel cell at 0 suns at night and gets supply from solar PV at 1 suns during day. The cell temperature is 25°C.

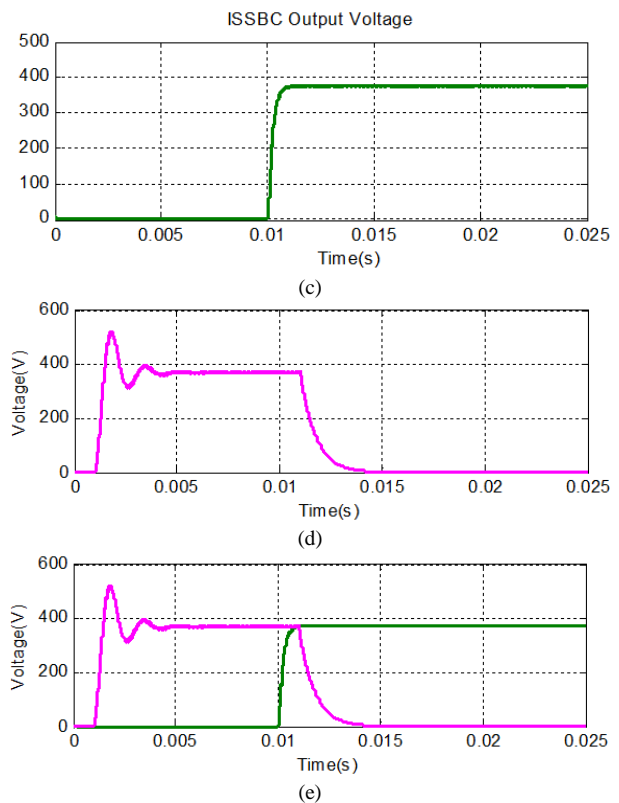
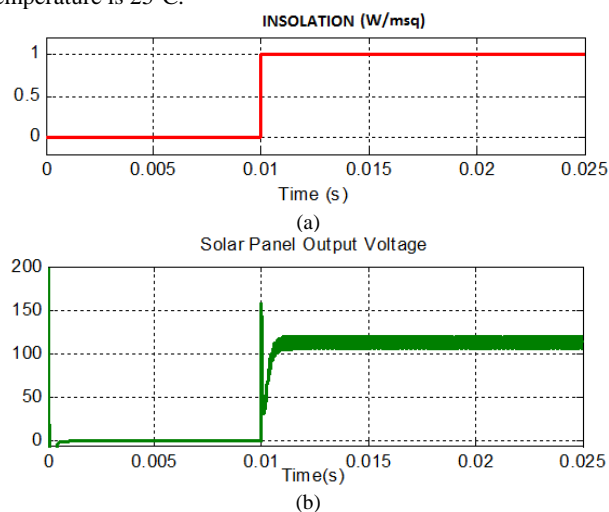


Figure 14: Insolation (b) PV voltage (c) ISSBC voltage (d) Fuel cell voltage (e) hybrid voltage

Both Fuel cell and solar PV are able to supply power to the load during day and night and DC link voltage is maintained as 370.07 V. It is shown in Figure 15. The Figures 16 (a-b) shows the fuel flow rate and air flow of the fuel cell respectively. From the figures, it is understood that at the time of no irradiation, the fuel flow rate gradually increases because of the operation of fuel cells and the same time, the stack efficiency of the fuel cell is high. The Figure 17 shows the torque curve of PMDC motor. The load gets continuous supply from the solar PV at 1 sun and from fuel cell at 0 suns. In both the conditions, the torque is maintained constant.

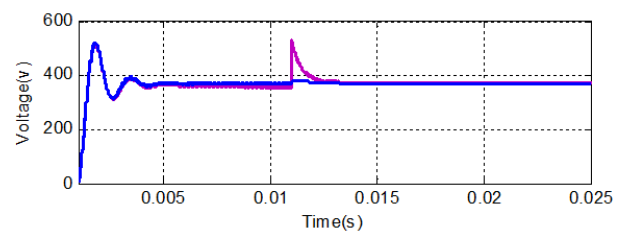


Figure 15: PMDC load voltage supplied by solar PV/fuel cell at day and night

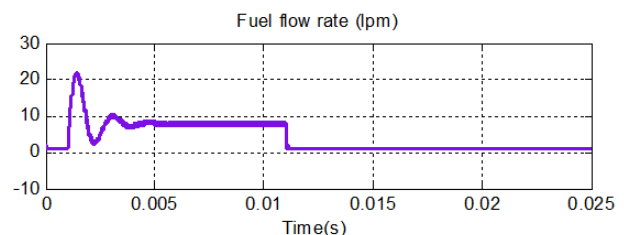
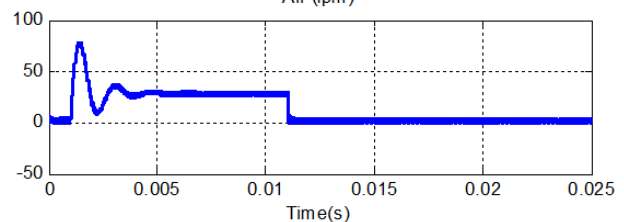


Figure 16
Air (lpm)



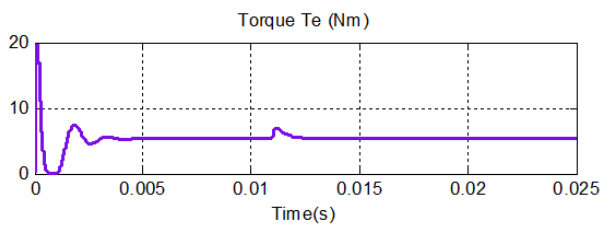


Figure 17: Torque curves of PMDC motor

5. Conclusion

The solar PV and fuel cell are used as a hybrid system in this work. To ensure the continuity of power supply during day and night, a solar PV with Fuel cell hybrid system has been proposed and control strategies are implemented. The result shows that the performances of both the sources are able to supply power to the load during day and night and DC link voltage is maintained as 370.07 V. Both solar PV module and fuel cell are able to maintain the torque of the motor around 2.681 Nm irrespective of the day and night conditions.

References

- [1] Elbaset AA, "Design, Modeling and Control Strategy of PV/FC Hybrid Power System", *Journal of Electrical Systems*, (2011), pp.270-286.
- [2] Borowy BS & Salameh ZM, "Methodology for Optimally Sizing the Combination of a Battery Bank and PV Array in a Wind/PV Hybrid System", *IEEE Transactions on Energy Conversion*, Vol.11, No.2, (1996), pp.367-375.
- [3] Rekioua D, Bensmail S & Bettar N, "Development of hybrid photovoltaic-fuel cell system for stand-alone application", *International journal of hydrogen energy*, Vol.39, (2014), pp.1604-1611.
- [4] Castaneda M, Cano A, Jurado F, Sanchez H & Fernandez LM, "Sizing optimization, dynamic modeling and energy management strategies of a stand-alone PV/hydrogen/battery-based hybrid system", *International Journal of Hydrogen Energy*, Vol.38, (2013), pp.3830-3845.
- [5] Ramakumar R, Abouzahr I & Ashenayi K, "A Knowledge-based Approach to the Design of Integrated Renewable Energy Systems", *IEEE Transactions on Energy Conversion*, Vol.7, No.4, (1992), pp.648-659.
- [6] Behzadi MS & Niasati M, "Comparative performance analysis of a hybrid PV/FC/battery stand-alone system using different power management strategies and sizing approaches", *International Journal of Hydrogen Energy*, Vol.40, (2015), pp.538-548.
- [7] Liu YH & Huang JW, "A fast and low cost analog maximum power point tracking method for low power photovoltaic systems", *Solar Energy*, Vol.85, (2011), pp.2771-2780.
- [8] El-Shatter TF, Eskandar MN & El-Hagry MT, "Technical note: Hybrid PV/fuel cell system design and Simulation", *Renewable Energy*, Vol.27, (2002), pp.479-485.
- [9] Chakrasali RL, Sheelavant VR & Nagaraja HN, "Network approach to modeling and simulation of solar photovoltaic cell", *Renewable and Sustainable Energy Reviews*, Vol.21, (2013), pp.84-88.
- [10] Mellita A, Benghanem M & Kalogirou SA, "Modeling and simulation of a standalone photovoltaic system using an adaptive artificial neural network: Proposition for a new sizing procedure", *Renewable Energy*, Vol.32, (2007), pp.285-313.
- [11] Chiang SJ, Shieh HJ & Chen MC, "Modeling and control of PV charger system with SEPIC converter", *IEEE Transactions on Industrial Electronics*, Vol.56, No.11, (2009), pp.4344-4353.
- [12] Bhatnagar P & Nema RK, "Maximum power point tracking control techniques: State-of-the-art in photovoltaic applications", *Renewable and Sustainable Energy Reviews*, Vol.23, (2013), pp.224-241.
- [13] Rajashekara K, "Hybrid Fuel-Cell Strategies for Clean Power Generation", *IEEE Transactions on Industry Applications*, Vol.41, No.3, (2005), pp.682-689.
- [14] Jia J, Li Q, Wang Y, Cham YT & Han M, "Modeling and Dynamic Characteristic Simulation of a Proton Exchange Membrane Fuel Cell", *IEEE Transactions on Energy Conversion*, Vol.24, No.1, (2009), pp.283-291.
- [15] Ulberg O, "Stand-alone power systems for the future: Optimal design, operation & control of solar-hydrogen energy systems", *University Of Zagreb*, (1998).
- [16] Dieguez PM, Ursua A, Sanchis P, Sopena C, Guelbenzu E & Gandia LM, "Thermal performance of a commercial alkaline water electrolyzer: Experimental study and mathematical modeling", *International Journal of Hydrogen Energy*, Vol.33, (2008), pp.7338-7354.
- [17] Tzimas E, Filiou C, Peteves SD & Veyret JB, "Hydrogen Storage: state-of-the-art and Future Perspective", *European Communities, Scientific and Technical Research series*, (2003).
- [18] Emayavaramban G & Amudha A, "Recognition of sEMG for Prosthetic Control using Static and Dynamic Neural Networks", *International Journal of Control Theory and Applications*, Vol.2, No.6, (2016), pp.155-165.
- [19] Emayavaramban G & Amudha A, "Identifying Hand Gestures using sEMG for Human Machine Interaction", *ARNP Journal of Engineering and Applied Sciences*, Vol.11, No.21, (2016), pp.12777-12785.
- [20] Ramkumar S, Sathesh Kumar K & Emayavaramban G, "EOG Signal Classification using Neural Network for Human Computer Interaction", *International Journal of Control Theory and Applications*, Vol.9, No.24, (2016), pp.223-231.
- [21] Ramkumar S & Hema CR, "Recognition of Eye Movement Electrooculogram Signals Using Dynamic Neural Networks", *KJCS*, Vol.6, (2013), pp.12-20.
- [22] Ramkumar S, Satheshkumar K & Emayavaramban G, "Nine States HCI using Electrooculogram and Neural Networks", *IJET*, Vol. 8, No.6, (2017), pp.3056-3064.
- [23] Ramkumar S, Sathesh Kumar K & Emayavaramban G, "A Feasibility Study On Eye Movements Using Electrooculogram Based HCI", *IEEE-International Conference on Intelligent Sustainable Systems*, (2017), pp.384-388.
- [24] Emayavaramban G, Ramkumar S, Amudha A & Sathesh Kumar K, "Classification of Hand Gestures Using FFNN and TDNN Networks", *International Journal of Pure and Applied Mathematics*, Vol.118, No.8, (2018), pp.27-32.